

Research Article

Practical Fingerprinting Localization for Indoor Positioning System by Using Beacons

Santosh Subedi and Jae-Young Pyun

Department of Information Communication Engineering, Chosun University, 375 Susuk-dong, Dong-gu, Gwangju, 501-759, Republic of Korea

Correspondence should be addressed to Jae-Young Pyun; jypyun@chosun.ac.kr

Received 23 June 2017; Revised 16 October 2017; Accepted 2 November 2017; Published 31 December 2017

Academic Editor: Eduard Llobet

Copyright © 2017 Santosh Subedi and Jae-Young Pyun. This is an open access article distributed under the Creative Commons Attribution License, which permits unrestricted use, distribution, and reproduction in any medium, provided the original work is properly cited.

Recent developments in the fields of smartphones and wireless communication technologies such as beacons, Wi-Fi, and ultra-wideband have made it possible to realize indoor positioning system (IPS) with a few meters of accuracy. In this paper, an improvement over traditional fingerprinting localization is proposed by combining it with weighted centroid localization (WCL). The proposed localization method reduces the total number of fingerprint reference points over the localization space, thus minimizing both the time required for reading radio frequency signals and the number of reference points needed during the fingerprinting learning process, which eventually makes the process less time-consuming. The proposed positioning has two major steps of operation. In the first step, we have realized fingerprinting that utilizes lightly populated reference points (RPs) and WCL individually. Using the location estimated at the first step, WCL is run again for the final location estimation. The proposed localization technique reduces the number of required fingerprint RPs by more than 40% compared to normal fingerprinting localization method with a similar localization estimation error.

1. Introduction

Though global positioning system (GPS) is very popular in localization applications, it is inefficient for indoor localizations [1]. Consequently, attention to indoor positioning system (IPS) has been increasing rapidly as an alternative to GPS for such locations. Various wireless technologies such as Bluetooth low energy (BLE), Wi-Fi, visible light communication (VLC), and ultra-wideband (UWB) have been used in IPS. Because BLE is widely supported by mobile devices and is designed for short-range wireless transmissions with low energy consumption and low cost, it seems more promising than other wireless technologies.

The main wireless signal measuring principles in IPS are time of arrival (TOA), time difference of arrival (TDOA), the angle of arrival (AOA), and received signal strength indication (RSSI). The TOA, TDOA, and AOA positioning systems require either proper time synchronization or an antenna array, which may increase the system cost. On the other hand, a RSSI-based positioning system

uses characteristics of wireless signal intensity over space and does not require time synchronization and angle measurement. Moreover, measurement of RSSI is relatively straightforward and can employ existing wireless technologies without any additional hardware devices, which eliminates extra cost and energy consumption. Most of the RSSI-based positioning research works use fingerprinting, trilateration, and triangulation methods as their basic techniques in IPS development. Among them, fingerprinting is adopted extensively because of its high degree of accuracy. However, the construction of an extensive reference point database during the offline phase makes fingerprinting time-consuming and labor intensive. The weighted centroid localization (WCL) method can also be a candidate technology for IPS. WCL is known as flexible, easy to implement, and consumes less time, but it has a large location estimation error [2, 3].

We present an IPS that reduces the number of reference points (RPs) for fingerprinting operations over localization space while yielding a location estimation error similar to

weighted k -nearest neighbor (Wk-NN) fingerprinting localization. The proposed localization uses BLE beacon-based fingerprinting, where the RSSI of beacons at the predetermined location and the location coordinates are stored in a database as an RP. Also, it uses collaboration between WCL and fingerprinting localization with fewer fingerprinting RPs.

This research paper is organized as follows. In Section 2, a brief review of typical IPS is presented. The proposed positioning system is elaborated upon in Section 3. Section 4 and Section 5 present experimental results and discussion and the conclusions of our research work, respectively.

2. Typical Indoor Positioning Systems

An IPS research work using BLE and fingerprinting is presented in [4] where Wk-NN positioning method is used. The k -nearest fingerprints are found in a database by using the Euclidean distance between the measured RSSI and the referred one from the database. This work also compares localization methods based on Wi-Fi and a combination of BLE and Wi-Fi.

Another work based on BLE beacon and fingerprinting techniques is introduced in [5] where a Gaussian filter is used to preprocess the receiving signals. Here, a distance-weighted filter based on the triangle theorem of trilateral relations is proposed to filter out the wrong distance value caused by an abnormal RSSI. Moreover, [6] proposes a hybrid approach to an integration of fingerprinting and trilateration with a gradient filter for RSSI estimation.

The WCL method is introduced in [7] for outdoor localization using a ZigBee-based sensor network. Theoretically, the WCL method is derived from a centroid determination process where weights are used to estimate positions. The weight being inversely proportional to a distance between the reference beacon location and an unknown current position plays a vital role in location estimation. Work using proprietary radio modules with the WCL method for tracking a person in a longwall mining application is presented in [8].

Radio signal strength- (RSS-) based fingerprinting positioning can also be integrated with motion sensor-based positioning. Such a system is put forward in [9] where the current position of the tag device is estimated by adding the previous position estimate and the position displacement from sensor-based positioning with the help of Kalman filter. An approach of using a user movement pattern and feeding this information to RSS-based localization system is reported in [10]. Here, recurrent neural networks are exploited to process RSS information to predict the user movement pattern. Meanwhile, RSS itself is not problem-free. It suffers a variance problem caused by environmental variations that are innate to both the training and test phase of fingerprinting localization. It is reported that even the same device without changing any experimental settings yields very different RSS characteristics [9, 11]. Reference [11] is a smartphone-based Wi-Fi fingerprinting system that tries to solve the RSS variation problem by assuming that there lies a linear shift in the

RSS values at training and test phase. Furthermore, with this assumption, peak RSS values from access points (APs) at RPs are stored and are used for localization in the test phase. Reference [9] adopts the concept of the linear shift in RSS values as proposed by [11] and try to mitigate the RSS variation problem. Here, the linear fitting parameters that represent the difference between the offline and online RSS observations are calibrated with recursive least square estimation (RLSE). Channel state information- (CSI-) based fingerprinting positioning can use amplitude and phase response of the Wi-Fi subcarriers and get rid of RSS [12]. Also, it is shown that CSI amplitude values exhibit good stability compared to RSS values. Here, feature-based fingerprints are generated with a deep learning approach.

2.1. Bluetooth Low Energy (BLE) Beacon. The specifications of Bluetooth version 4.0 [13] released in June 2010 introduced a new technology called Bluetooth low energy (BLE) or “Bluetooth Smart.” In this version, among the two lowest layers of the BLE stack, the physical (PHY) layer takes care of transmitting and receiving bits, whereas the link layer (LL) provides medium access, connection establishment, error control, and flow control. As with the other protocols defined in BLEs, logical link control and adaptation protocol (L2CAP), generic attribute protocol (GATT), and generic access profile (GAP) operate on the upper layers.

Indeed, BLE is designed for devices that do not require large amounts of data transfer and is intended for short-range wireless transmission with low energy consumption and cost [14, 15]. A research work presented in [16] has reported that the power draw of the mobile device (tag) is lower for BLE than for Wi-Fi.

For the transmission, BLE operates at an industrial, scientific, and medical (ISM) frequency band of 2.4 GHz. The frequency band is divided into 40 channels spaced at 2 MHz apart. Among the 40 channels, three channels are used for an advertisement. A BLE device uses these advertisement channels to broadcast its advertisement packets continuously. Moreover, these three advertising channels are strategically placed to avoid interference with coexisting technologies like IEEE 802.11 and ZigBee [17].

A BLE device deployed in IPS is called a “beacon.” Recently, many companies have emerged that provide beacons commercially. We used Estimote Beacon devices as BLE beacons in our experiment [18].

2.2. Weighted Centroid Localization (WCL). In the WCL method for location estimation, weight (w_i) is assigned to beacons when measuring the distance from a tag device. The weight is the inversed distance applied to a degree (g). The main advantage of this method is that it always confines location estimation inside the region surrounded by beacons. Moreover, any beacon near the tag device will have the highest weight, so that the final location estimation is pulled towards this beacon. For m beacons, WCL is defined by the following set of equations:

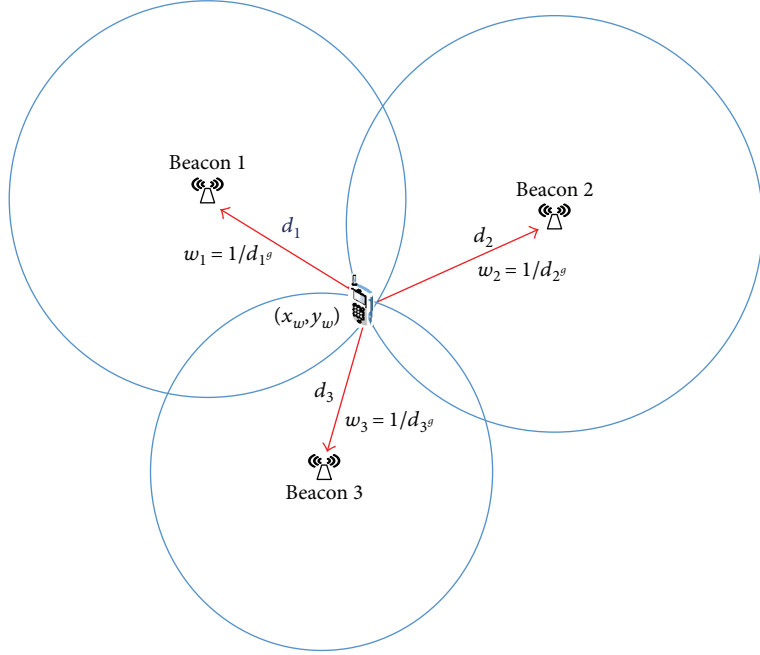


FIGURE 1: Example for weighted centroid localization.

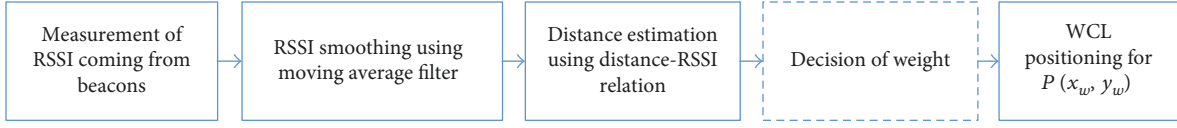


FIGURE 2: The operation procedure of a weighted centroid localization- (WCL-) based positioning system. Box with dotted lines represents work we added for our proposed positioning method.

$$\begin{aligned} x_w &= \sum_{i=1}^m x_i \times \frac{w_i}{\sum_{i=1}^m w_i}, \\ y_w &= \sum_{i=1}^m y_i \times \frac{w_i}{\sum_{i=1}^m w_i}, \\ w_i &= \frac{1}{d_i^g}, \end{aligned} \quad (1)$$

where (x_w, y_w) is the estimated coordinate of the WCL method, d_i is distance between the tag and beacon i , g is the degree of weight [2], and m is the total number of beacons considered at any time for location estimation. Some typical values of g are 0.5, 1, and 2.6 [2, 3, 8]. For example, Figure 1 illustrates WCL with three beacons within the localization area. At first, distances (d_1 , d_2 , and d_3) from beacons to the tag device are estimated using the log distance propagation model and respective weight is decided depending on both those distances and degree (g).

The flowchart shown in Figure 2 depicts the operation of the WCL positioning system. The operation procedure starts with the measurement of raw signal strength coming from the deployed beacons. These signals are further smoothed using a moving average filter.

2.3. Fingerprinting Localization. Fingerprinting is the most popular method of localization because of its high accuracy compared to other methods. It does not require line-of-sight measurements of APs, has low complexity, and gains high applicability in the complex indoor environment [12, 19]. Fingerprinting-based localization usually consists of two main phases: offline (training) and online (test).

2.3.1. Offline Phase. The offline phase of fingerprinting is designed for learning the RSSI at each reference point. At this stage, we collect RSSIs from all beacons. RSSIs in four directions (0° , 90° , 180° , and 270°) at each measurement location are collected as shown in Figure 3. These collected RSSIs are stored in a database along with their location coordinates, which are called reference points (RPs) in this paper.

2.3.2. Online Phase. In the online phase, RSSIs from beacons are measured and compared with the stored ones in the database. Then, the location of the tag device is estimated using the fingerprinting procedure described in Figure 4. The positioning distance (D_j) between the stored RSSI value

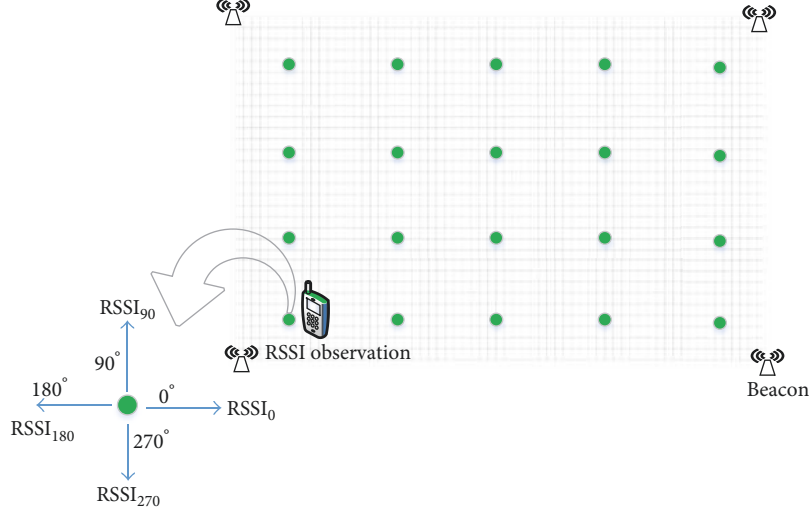


FIGURE 3: The offline phase of fingerprinting localization. The green dots are reference points, and RSSI_0 represents RSSI value at 0° to the reference direction.

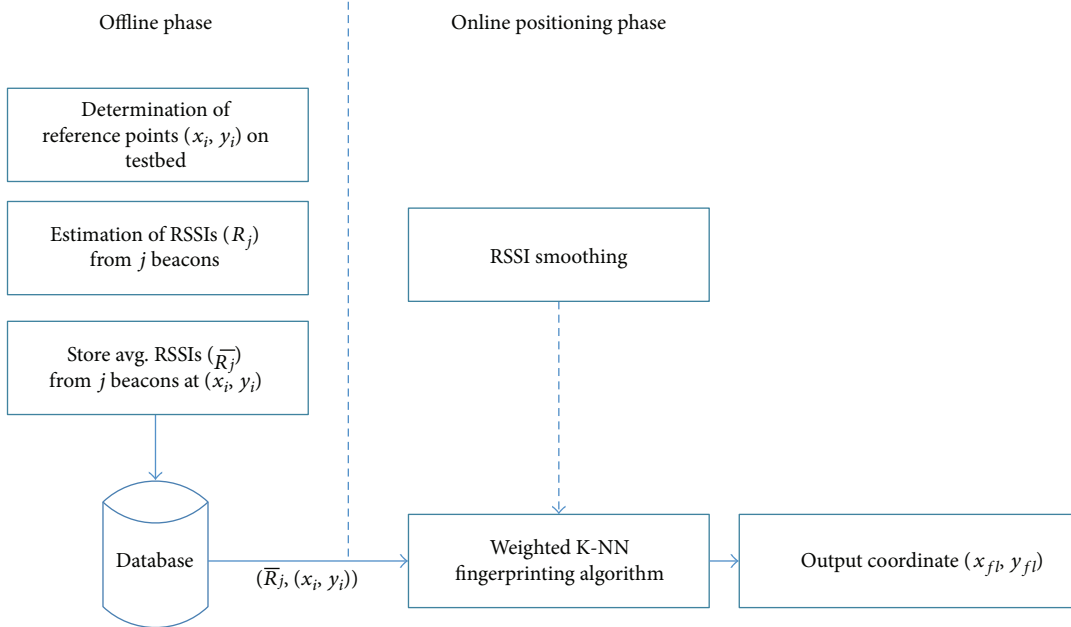


FIGURE 4: The process flow of fingerprinting localization method.

$(\text{RSSI}_{\text{offline}})$ and the online collected RSSI value ($\text{RSSI}_{\text{online}}$) at j th reference point is given by

$$D_j = \sum_{i=1}^m \sqrt{(\text{RSSI}_{i_{\text{online}}} - \text{RSSI}_{i_{\text{offline}}})^2}, \quad (2)$$

where i is the number of beacons ranging from 1 to m , the total number of beacons around the tag. Here, Wk-NN can be used as a matching algorithm based on stored and online RSSI values [4, 20, 21]. In order to determine weight of any reference point, D_j is sorted in an ascending order. Least k positioning difference is chosen, and inverse of it is assigned as weight to their respective reference points.

3. The Proposed Positioning System

In the arena of indoor location positioning techniques, fingerprinting has been a prime choice for researchers due to its good estimation. However, the inevitable drawback of this method is the requirement of a tedious and time-consuming offline phase. Also, though WCL seems easy and flexible to implement, it has a high localization error [2]. The proposed system starts with the removal of noisy RSSI values followed by the proposed positioning method explained below.

3.1. Filtration of Measured RSSI. Due to several noise factors and attenuation, RSSI exhibits high variability in space and

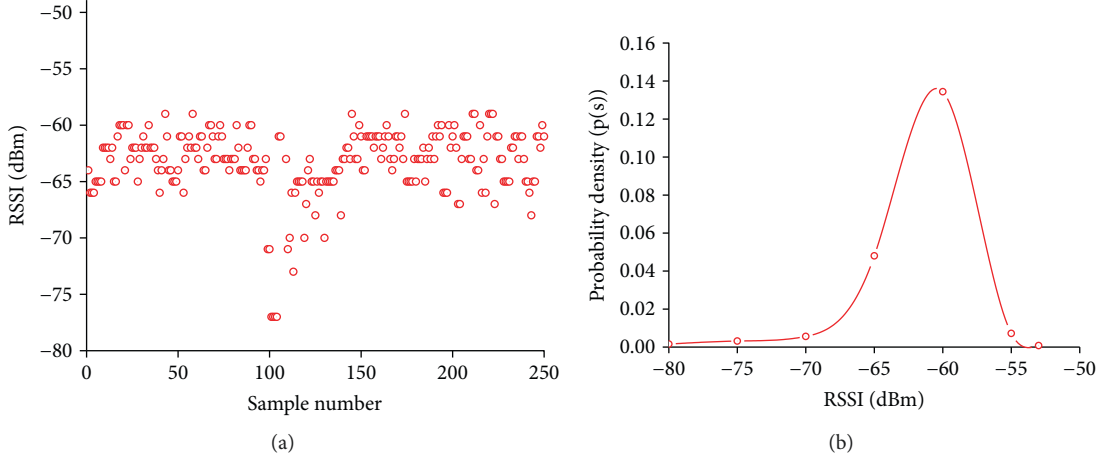


FIGURE 5: Distribution of RSSI at a certain point. (a) Fluctuation of RSSI values and (b) Gaussian probability distribution.

time [9, 11]. That is, RSSI at a tag device fluctuates over time. Hence, it is important to find the correct RSSI values that eventually help to reduce the estimation error. For that reason, in this study, we have utilized a Gaussian filter to estimate RSSI values in training or offline phase and the moving average filter for smoothing the real-time RSSI in test or online phase.

3.1.1. Gaussian Filter for Training Data. The distribution of RSSI at a particular point can be thought as a Gaussian distribution [5, 22]. We perform statistical distribution of RSSI at our testbed as shown in Figure 5. As depicted in Figure 5, since the Gaussian distribution can represent the randomness of RSSI in a real environment, we use a Gaussian filter for estimating the value of RSSI to construct radio map database in the training phase. The mean (μ) and variance (σ^2) of Gaussian filter are given as follows:

$$\begin{aligned} \mu &= \frac{1}{N} \sum_{n=1}^N \text{RSSI}_n, \\ \sigma^2 &= \frac{1}{N-1} \sum_{n=1}^N (\text{RSSI}_n - \mu)^2, \end{aligned} \quad (3)$$

where n is the number of samples.

Now, the probability density function is formulated as

$$f(\text{RSSI}) = \frac{1}{\sigma\sqrt{2\Pi}} e^{-(\text{RSSI}-\mu)^2/\sigma^2}. \quad (4)$$

We accept the centralized RSSI values (68.2%) that lie in the effective range of $\mu + \sigma$ and $\mu - \sigma$. The RSSI is estimated by averaging the values that are in the effective range.

3.1.2. Moving Average Filter for Smoothing RSSI. As shown in Figure 5, the randomness of RSSI can lead to significant variation in RSSI value. Hence, it is mandatory to smooth the real-time-received RSSI for reducing the probable localization error. The moving average filter can be explained as follows:

Let us consider the following dataset.

$$\text{RSSI}_0 = [\text{RSSI}_0(1), \text{RSSI}_0(2), \dots, \text{RSSI}_0(n)], \quad (5)$$

where $\text{RSSI}_0(n)$ corresponds to the n th RSSI observed around the tag device.

Now, a set of the last ten elements in (5) is taken and averaged as follows:

$$\text{RSSI}_1 = [\text{RSSI}_1(1), \text{RSSI}_1(2), \dots, \text{RSSI}_1(n-9)], \quad (6)$$

where $\text{RSSI}_1(k) = \sum_{m=k}^{k+9} \text{RSSI}_0(m)$ and $k \geq 1$. Here, when the number of RSSI sample is less than 10, we take average of all the samples; hence, there will not be any delay in real-time position estimation.

The result after using the moving average filter is shown in Figure 6.

3.2. Distance Observation from RSSI. After the RSSI estimation, it is converted to distance using the following relation between distance and received power [2, 23].

$$P_r(d)[\text{dBm}] = A - 10n \times \log_{10}(d), \quad (7)$$

where $P_r(d)$ is the received RSSI in dBm at distance d , A is the received RSSI at one meter, and n is the path loss exponent.

3.3. The Proposed Positioning Method. The proposed technique integrating two different localization technologies contains two major steps of operation. At the first stage of operation, both fingerprinting, with lightly populated reference points over testbed (we call it FP_{light} in the rest of the paper), and WCL localizations perform individually. That is, the coordinates estimated from FP_{light} and WCL are obtained. These estimated coordinates and their respective measured distances are further processed in the next WCL operation as the second step of the procedure. As we know, in weighted k -nearest neighbor fingerprinting localization, a certain weight is assigned to

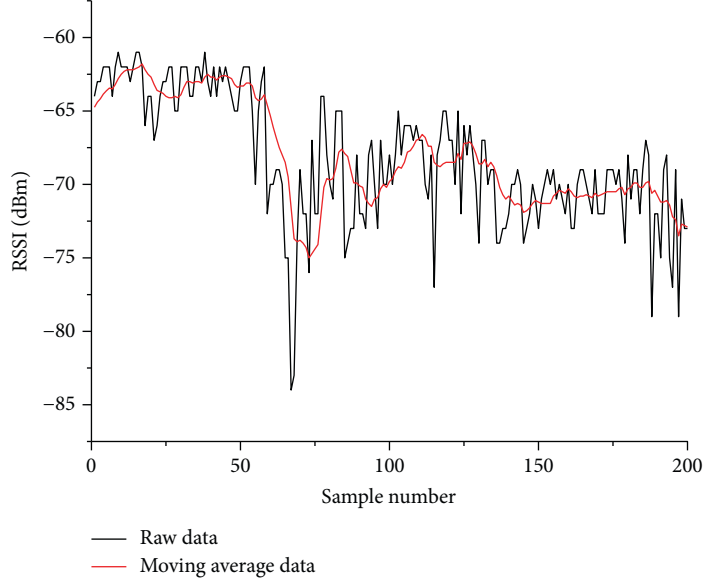


FIGURE 6: RSSI smoothing using moving average filter.

“ k ” nearest neighbor depending on their Euclidean distance to observed online value. In our method too, we locate “ k ” nearest neighbor depending on observed online value. However, the weights of these nearest neighbors are determined depending on their Euclidean distance to first WCL coordinate estimation.

In brief, the proposed practical fingerprinting method combines WCL and traditional fingerprinting localization while using lightly populated reference points to cover the whole area of interest. The fingerprint data formed by a site survey in a Wk-NN fingerprinting method can be summarized as follows:

$$\text{Fingerprint}_{\text{data}} = \begin{bmatrix} \text{RSSI}_{B_1}(\text{RP}_1) & \text{RSSI}_{B_2}(\text{RP}_1) & \dots & \text{RSSI}_{B_M}(\text{RP}_1) \\ \text{RSSI}_{B_1}(\text{RP}_2) & \text{RSSI}_{B_2}(\text{RP}_2) & \dots & \text{RSSI}_{B_M}(\text{RP}_2) \\ \vdots & \vdots & \ddots & \vdots \\ \text{RSSI}_{B_1}(\text{RP}_N) & \text{RSSI}_{B_2}(\text{RP}_N) & \dots & \text{RSSI}_{B_M}(\text{RP}_N) \end{bmatrix}, \quad (8)$$

where $\text{RSSI}_{B_1}(\text{RP}_1)$ represents RSSI from beacon B_1 at RP₁ with M and N being the total number of deployed beacons and total RPs on the testbed, respectively. Depending on the value of M and N , the size of fingerprint datasets varies accordingly. Here, the proposed method tries to minimize N , keeping the localization accuracy similar to the existing system.

On the testing phase of the proposed method, RSSI of the deployed beacons is smoothed using the moving average filter. Among these beacons, any m numbers of beacons are selected based on the strongest RSSI value. Distances from the tag device to these m beacons are estimated for the WCL method. To consider the beacon deployment in a rectangular fashion and to decrease the possible localization error, four beacons are selected in our work. In the proposed

technique illustrated in Figure 7, WCL and FP_{light} (selects k RPs with small distances to test data) methods are run in the first step. While implementing Wk-NN, authors usually recommend different values for k such as $k = \{2\}$ [4] and $k = \{3, 4\}$ [24]. In our method, we observed that while $k = \{4, 5\}$ is considered, the reference points located far from the original tag position also get selected (because of a larger space between the two reference points) and increase the localization error. We got the least localization estimation error with $k = 3$. Hence, the value of k is set to 3 in our work, such that the three nearest possible RP locations are estimated. It is noteworthy that, in a conventional fingerprinting positioning, a high space between two RPs reduces granularity or accuracy of the positioning system and a small space increases accuracy. However, the small space between the RPs does not increase the probability of correctly matching the fingerprints because close reference points may have very similar fingerprints [25].

We have strategically chosen the total number of RPs and space between them to reduce the localization error as illustrated in Section 4. For the sake of uniformity, the height of the tag device is kept as 1.20 m from the ground in “Messaging/testing” position (the usual way of holding smartphone) in both the training and test phase.

Figure 8 illustrates the process flow of the proposed method. Here, WCL_1 and WCL_2 represent WCL operation with two different input data sets. WCL_1 operates with the beacons to tag distances and their respective weights (as explained in Section 2.2). Similarly, WCL_2 works with the newly calculated distances and their respective weights.

Let the estimated locations by WCL_1 and FP_{light} (three RPs) be (x_w, y_w) , (x_{f1}, y_{f1}) , (x_{f2}, y_{f2}) , and, (x_{f3}, y_{f3}) , respectively, as illustrated in Figure 9. Euclidian distances between WCL and FP_{light} estimated locations are calculated as shown in (9).

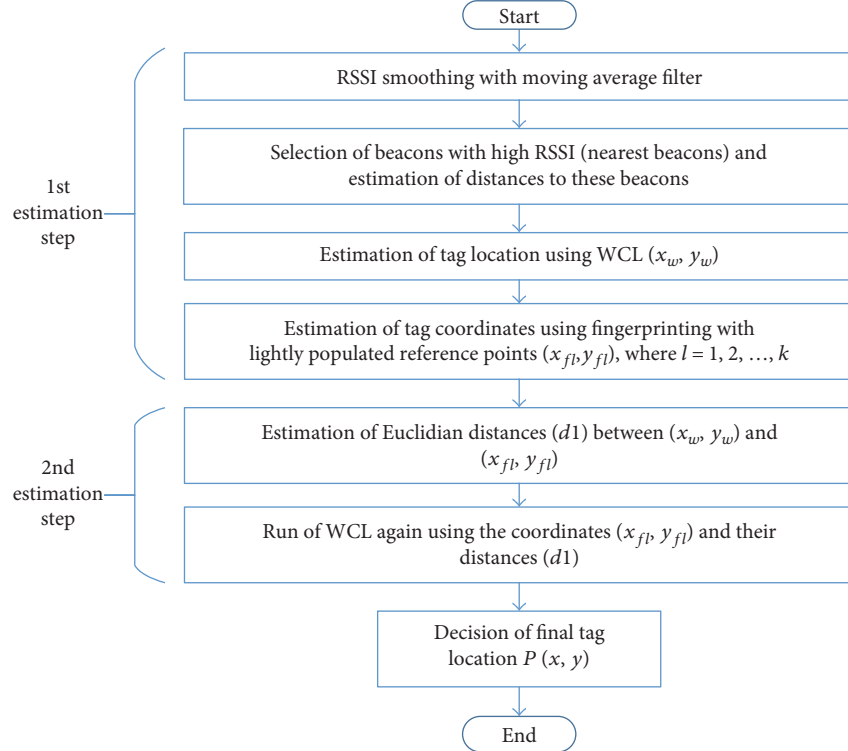


FIGURE 7: Working procedure for the proposed fingerprinting localization.

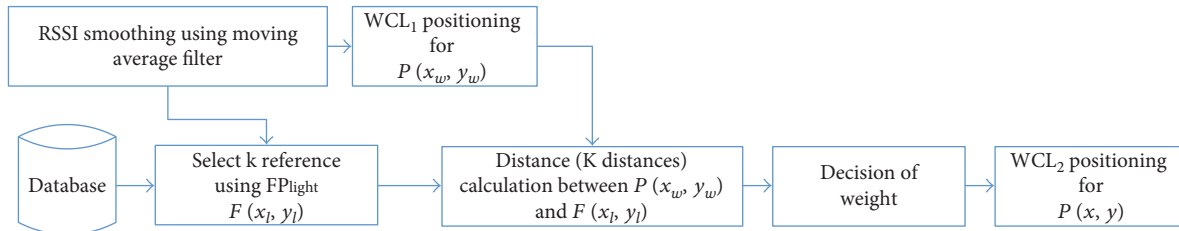


FIGURE 8: The process flow of the proposed localization method.

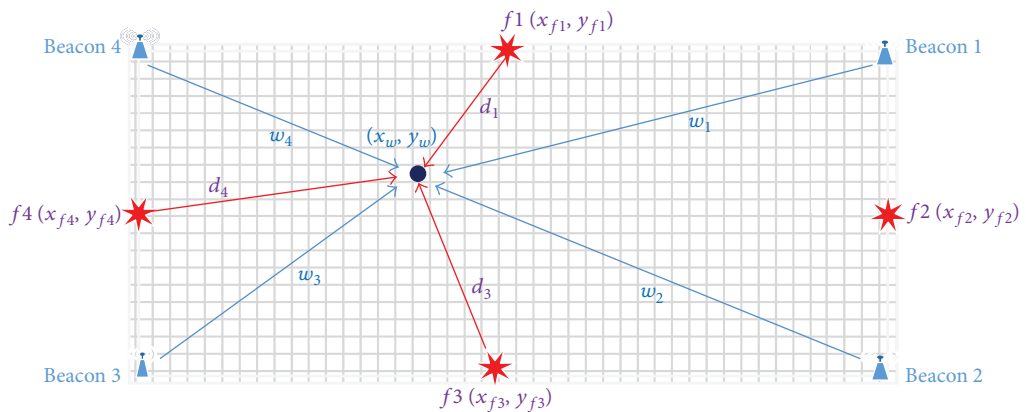


FIGURE 9: Localization estimation of the proposed method.

$$d_l = \sqrt{(x_w - x_{fl})^2 + (y_w - y_{fl})^2}, \quad (9)$$

where (x_w, y_w) and (x_{fl}, y_{fl}) refer to the coordinates obtained from WCL and FP_{light}, respectively, and $l=1, 2, \dots, k$.

Now, the above three calculated distances are converted to their respective weights as in the WCL method using degree (g). Further, in the second step shown in 10, the three estimated locations by FP_{light} $((x_{f1}, y_{f1}), (x_{f2}, y_{f2}),$ and $(x_{f3}, y_{f3}))$ and their respective calculated weights (w_1 , w_2 , and w_3) are used for the second WCL estimation (WCL₂). The output of WCL₂ estimation is the final location estimation of our proposed method.

$$P(x, y) = \left(\frac{\sum_{l=1}^k x_{fl} \times w_l}{\sum_{l=1}^k w_l}, \frac{\sum_{l=1}^k y_{fl} \times w_l}{\sum_{l=1}^k w_l} \right), \quad (10)$$

$$w_l = \frac{1}{d_l^g}.$$

4. Experimental Results and Discussion

For the proper evaluation of the proposed method, we tested the proposed positioning method by conducting experiments at the corridor and the room.

4.1. Testbed 1 (Corridor). The beacons are deployed in a rectangular form with an orientation towards their opposite walls at the corridor. For the WCL technique, the four nearest beacons are selected by their RSSIs. WCL has two main localization properties: (a) The estimated location is confined inside the location of the beacons, and (b) It drags the location estimation towards the nearest beacon from the moving user. Keeping these properties in mind, we choose different distinct regions across the corridor for localization measurement purposes. Therefore, measurements are taken both at the border of the rectangular polygon formed by beacons and at central regions of the polygon. Moreover, in any region, measurements are taken at three different places as shown in Figure 10, such as away from the wall (A), midway of the corridor (B), and near the wall (C). Also, the degree value can be adjusted for best positioning result in WCL. If g is kept high, the localization estimation moves to the closest anchor position. On the other hand, very low value (near to zero) may also yield the localization estimation as a centroid point. Hence, we evaluated the localization estimation error of WCL with different values of g (0.4, 0.5, 0.8, and 1.2) in our testbed as shown in Figure 11. At a measurement place, 100 measurements are taken and the location estimation error is averaged. Table 1 gives the glimpse of experimental condition at the corridor.

As shown in Figure 11, the performance of the WCL method with degree 0.5 is better than others in our testbed. Therefore, the WCL method with degree 0.5 is used for the proposed fingerprinting process. With this beacon deployment configuration, the proposed localization technique is implemented at the corridor. Then, we evaluate the

performance of our method with various numbers of reference points over the testbed.

At first, we took 12 reference points such that there was a reference point in between any two beacons along the corridor. Later, we increased the number of reference points uniformly over the testbed to 19, 26, and 36, as depicted in Figure 12. We compared our proposed fingerprinting with weighted K-NN fingerprinting localization. For this, since we are confined to two opposite walls of the corridor, we divided the testbed into 62 uniform grids of length 1.25 m and breadth 0.9 m, forming 62 fingerprinting reference points or radio map cells. Wk-NN fingerprinting was also performed using 36 reference points intended for the proposed practical fingerprinting localization. The value of k is set to 4 for better localization estimation in Wk-NN fingerprinting.

At first, we observed the cumulative distribution function (CDF) of the localization estimation error at a fixed point in testbed by various positioning methods. Since the proposed method with 12 and 19 reference points have a very high location error, we excluded them in this observation. The CDF of the localization estimation error at the corridor is given in Figure 13.

For an exhaustive study, a location error is estimated at three regions: (i) the center of the polygon formed by beacons, (ii) the border of the rectangular polygon, and (iii) the edge of the corridor or end of beacon deployment as shown in Figure 14. Similar to the WCL location error estimation, at each region, location error is estimated at three different places (A, B, and, C). At each measurement place, we took 200 samples of location estimation error, with 50 samples in each direction (0°, 90°, 180°, and 270°).

In Figures 15, 16, and 17, the mean localization error of the proposed practical fingerprinting (PF) localization method in different measurement regions and measurement places is compared with Wk-NN fingerprinting and WCL. Since the high space between the two reference points reduces granularity in normal fingerprinting localization, the proposed positioning result is compared to Wk-NN fingerprinting with 36 and 62 reference points only.

As shown in Figure 15, the proposed method with less number of RPs (12 and 19) or high space among reference points results to a high positioning error. At this condition, the performance of WCL is better than the proposed method. It is so because, at the edge of the corridor, the selected three nearest RPs are far away from the measurement place. However, PF with 36 RPs yields a localization error similar to Wk-NN fingerprinting localization.

Figure 16 shows the location estimation error at three measurement places (A, B, and C) in the border region of the rectangular polygon. Here, the PF with 36 RPs has almost similar or lesser localization error to Wk-NN fingerprinting with 62 reference points. However, the positioning result with the lesser number of RPs has a high mean error. The positioning error of the proposed method with 36 and 26 RPs has less difference as compared to that of PF with 19 and 12 RPs. It is so because the border region contains RPs' location that can be utilized for PF with 26 RPs (see Figure 12). It is also observed at the edge of the corridor (see Figure 15). A similar result follows at the center of the



FIGURE 10: Experimental environment: beacons deployed in the corridor where blue circular dots along the wall of the corridor represent beacon deployment positions, and measurement places are marked on the floor as A, B, and C.

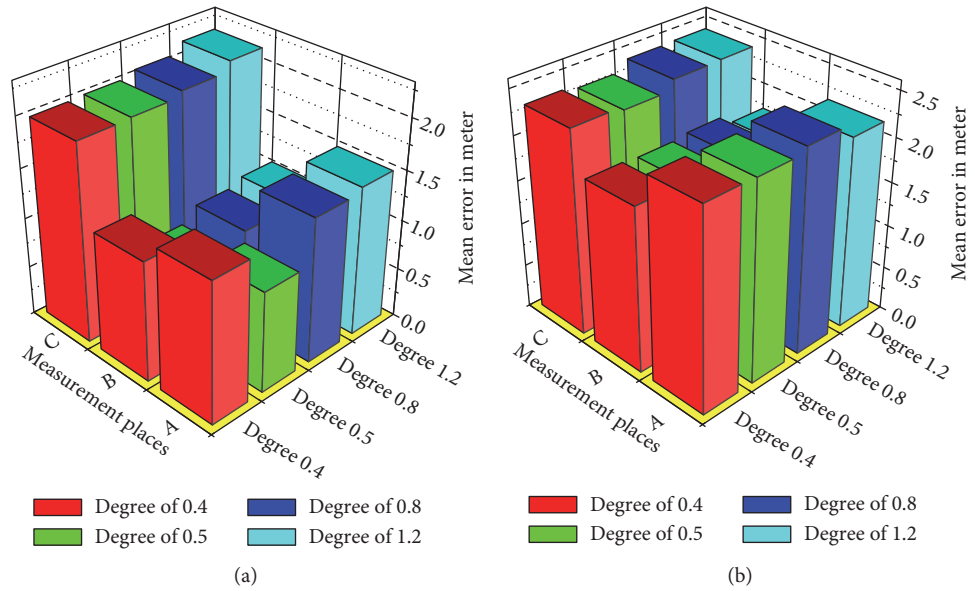


FIGURE 11: Average location error at different measurement places (A, B, and C) in the (a) central and (b) border regions of a rectangular polygon with a respective degree of weight.

TABLE 1: Experiment conditions for the evaluation of the proposed fingerprinting method at the corridor.

Parameters	Value
Total number of beacons (M)	14
Space between two adjacent beacons	4.5 m
Breadth of corridor	2.5 m
Height of beacon deployment	2.5 m
Beacon transmission power	+4 dBm
Beacon advertisement interval	300 milliseconds
Tx-Rx devices	Estimote beacons, iPhone 4S
$A[\text{dBm}]$	-60.85
Path loss exponent (n)	1.3
Degree (g) in WCL method	0.5
Number of reference points (N)	12, 19, 26, and 36

rectangular polygon as shown in Figure 17. Here, the k -nearest RPs are far away for PF with 26 and 19 RPs. Therefore, they yield more localization errors.

Furthermore, in all regions of the corridor, the location estimation error is lower at the midway (measurement place B) and higher near the walls. This condition has less effect for real indoor positioning applications because people tend to walk down the middle of the corridor and avoid the places near the walls. The lowest and highest average errors obtained in testbed 1 are 0.8679 m and 1.14 m, respectively. While using the proposed method with 36 reference points across the testbed 1, we can reduce the number of reference points by 41.93%.

4.2. Testbed 2 (Room). The experimental conditions for evaluation of the proposed method at the testbed 2 are listed in Table 2.

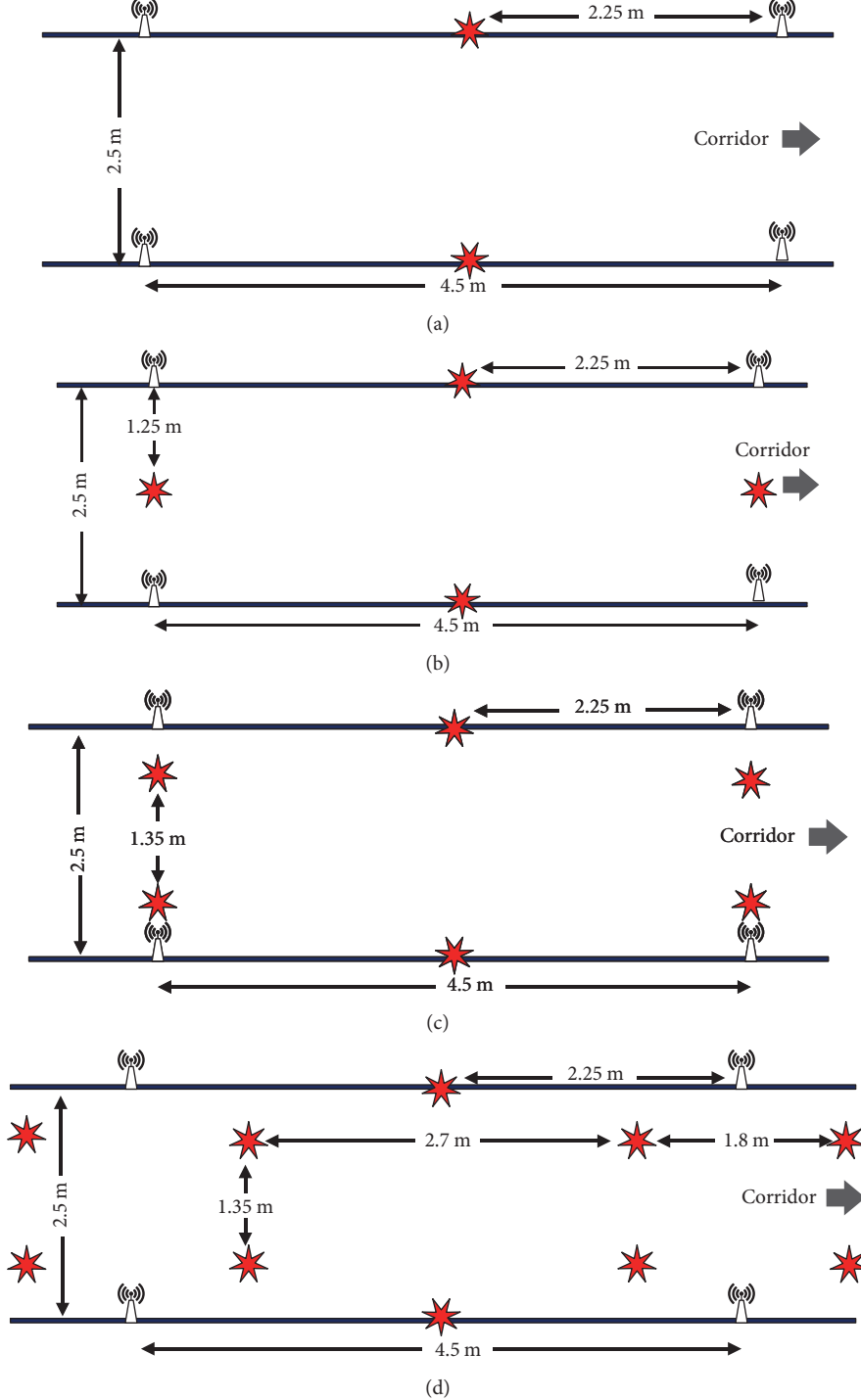


FIGURE 12: Testbed conditions for fingerprinting positions of (a) 12, (b) 19, (c) 26, and (d) 36 reference point distribution pattern over the testbed where red stars represent reference points.

Here, beacons are deployed at the four corners and center of the room. In WCL, shorter distances are more weighted than higher distances for a fixed value of the degree (g). Hence, to weight longer distances marginally lower, g is kept high [7]. However, in our case, beacon deployment height is almost the same in both testbeds. Moreover, distance from the tag device to the beacon is also

in a similar range during the operation. Hence, we choose the value of g as 0.5 in the room too. Although, beacon density per unit area in the room is much lower than that in the corridor, all the beacons in the room are much closer to each other.

Since we are not constrained by two walls as in the corridor, we divided the testbed 2 into a uniform grid with 65 cells

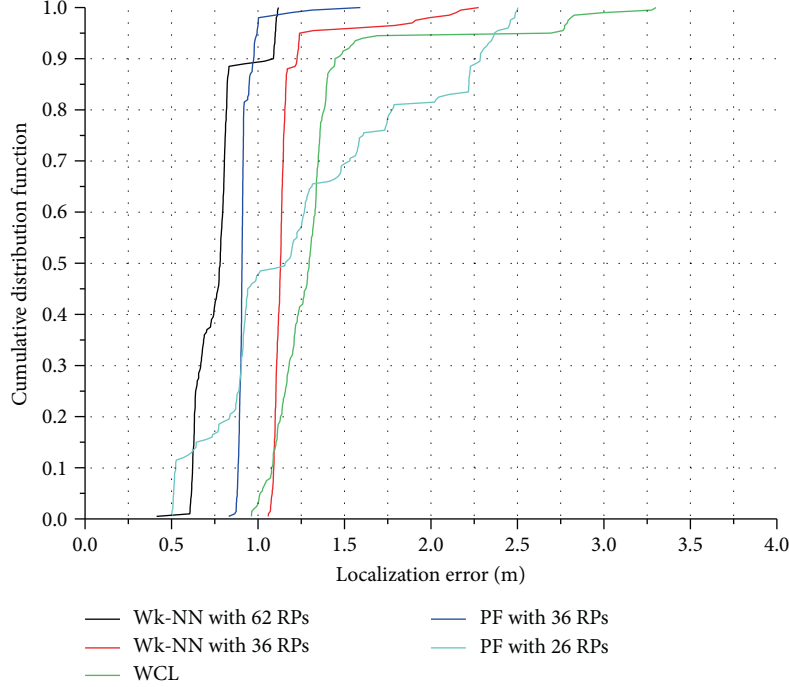


FIGURE 13: CDF of the localization estimation error at a fixed place in the testbed 1.

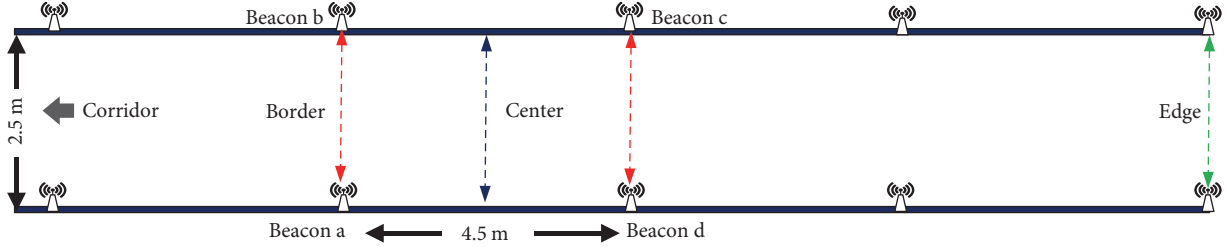


FIGURE 14: Location error measurement regions in the testbed 1 where any four adjacent beacons form a rectangular polygon (e.g., the rectangle formed by beacons a, b, c, and d). The red, blue, and green lines indicate the border of the polygon, the center of the polygon, and the edge of the corridor, respectively.

of length and breadth 0.9 m for evaluation of Wk-NN fingerprinting. Furthermore, we increased the size of the grid to 1.35 m and 1.8 m forming 28 and 16 fingerprinting reference points, respectively. Also, to mitigate the high location error of WCL near the walls, we added one more reference point in the middle of each wall. Therefore, the proposed fingerprinting method is evaluated using 20 and 32 reference points in the testbed 2. Following the localization error variation of WCL, location error is estimated at three measurements places inside the testbed room as shown in Figure 18.

The CDF of the location estimation error by various positioning methods at a fixed point in the testbed 2 is presented in Figure 19.

A detailed study is done by examining the location estimation error at three different measurement places inside the testbed room as shown in Figure 20.

Figure 20 shows the mean localization error comparison between the proposed method and existing localization

methods Wk-NN fingerprinting and WCL. Due to the fully furnished testbed condition, localization error is higher in the room than in the corridor. Measurement place A is the center of the room where the localization error of WCL method is least. It is so because, at this measurement place, a beacon is just above the tag device and the remaining four beacons are almost at an equidistance to this place. Since a beacon is very near to the tag device, it has high weight, and the remaining beacons have relatively low weight. Measurement place C is near a wall of the room, and measurement place B is midway between the wall and center of the room. PF with 32 RPs closely follows the mean localization error of Wk-NN everywhere. However, PF with 20 RPs yields a large localization error due to the large distance between the RP locations. Similar to the corridor, the localization error is increased as we move towards the wall of the room.

As expected, Wk-NN with 65 reference points has the lowest localization error throughout the room whereas this

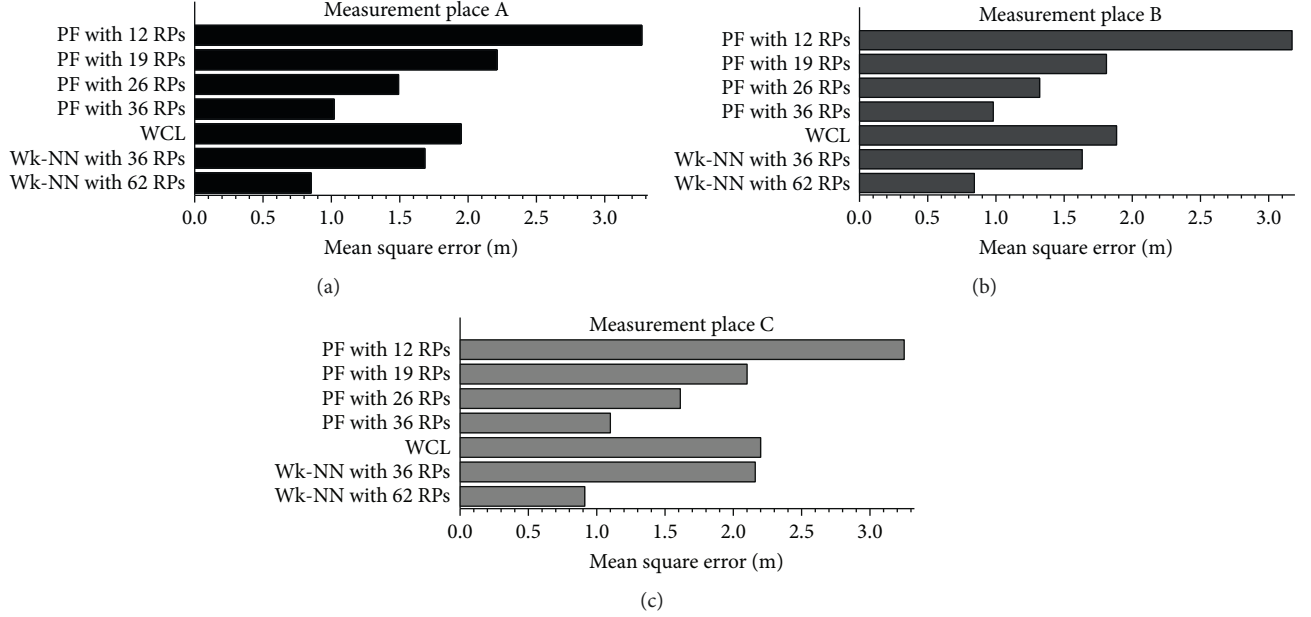


FIGURE 15: Average location error at different measurement places at the edge of the testbed corridor: (a) measurement place A, (b) measurement place B, and (c) measurement place C. PF: proposed practical fingerprinting; Wk-NN: weighted k -nearest neighbor; WCL: weighted centroid localization; RF: reference points.

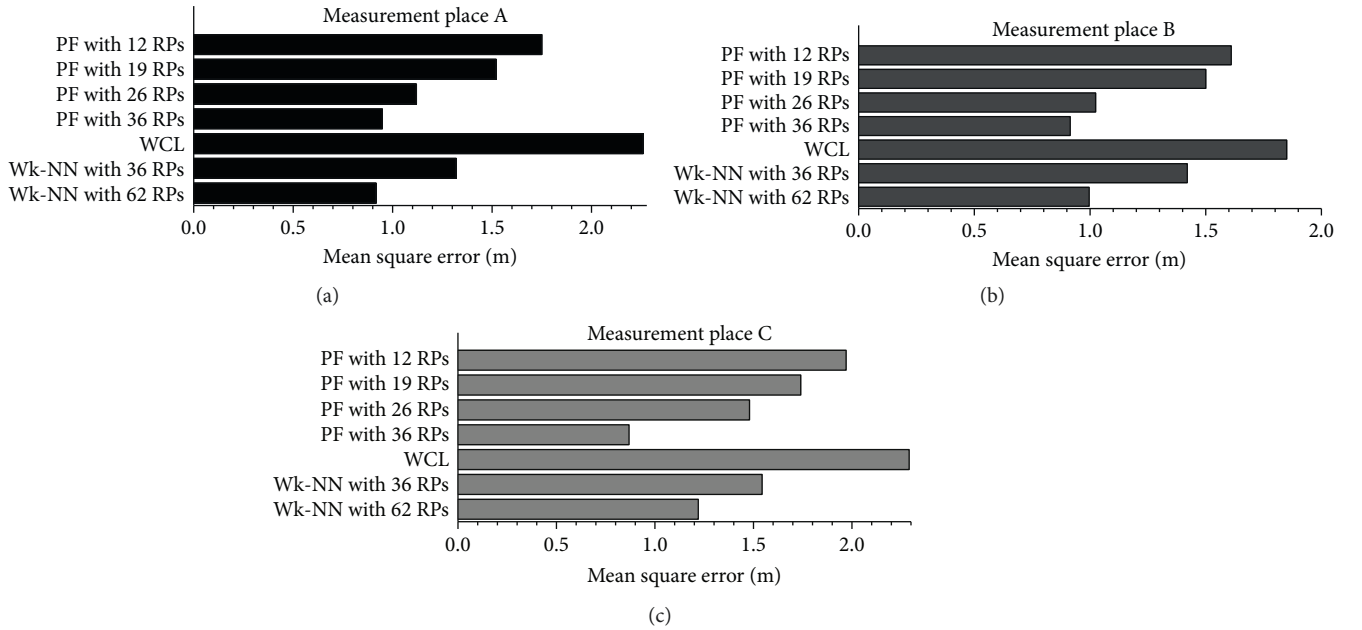


FIGURE 16: Average location error at different measurement places at the border of the rectangular polygon: (a) measurement place A, (b) measurement place B, and (c) measurement place C. PF: proposed practical fingerprinting; Wk-NN: weighted k -nearest neighbor; WCL: weighted centroid localization; RF: reference points.

method with 32 reference points has a high localization error due to the larger size of the grid. However, the proposed method takes the benefit of coarse localization estimation of WCL and yields a better result. The lowest and highest average errors obtained by the proposed method (32 reference points) in testbed 2 are 0.9893 m and 1.5529 m, respectively. While using the proposed method with 32 reference points

across the testbed 2, we can reduce the number of reference points by 49.23%.

4.3. Statistical Validation of the Presented Result. To validate the reported result, we perform Friedman as the ranking test [26, 27] and Holm [28] as the post hoc test. For the test, we set the null hypothesis (H_0) as

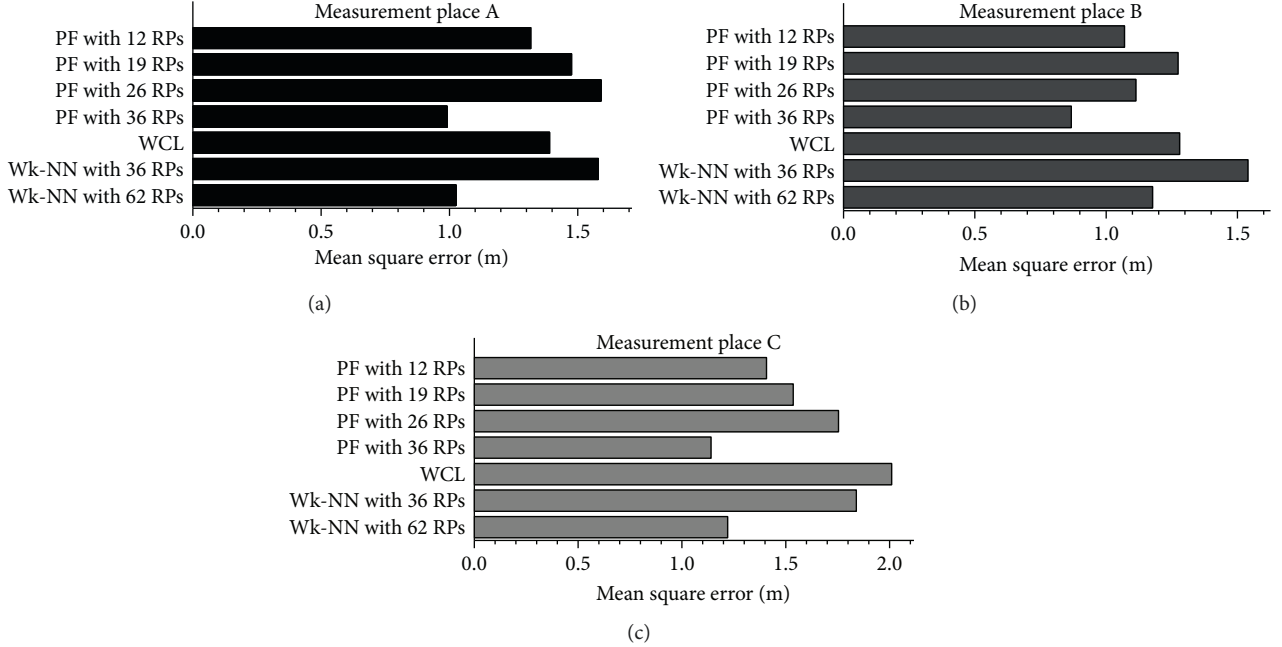


FIGURE 17: Average location error at different measurement places in the center of the rectangular polygon: (a) measurement place A, (b) measurement place B, and (c) measurement place C. PF: proposed practical fingerprinting; Wk-NN: weighted k -nearest neighbor; WCL: weighted centroid localization; RF: reference points.

TABLE 2: Experiment conditions for the evaluation of the proposed fingerprinting method at the room.

Parameters	Value
Total number of beacons (M)	5
Length/breadth of the room	7.28 m \times 7.24 m
Height of beacon deployment	2.7 m
Beacon transmission power	+4 dBm
Beacon advertisement interval	300 milliseconds
Tx-Rx devices	Estimote beacons, iPhone 4S
A [dBm]	-64.97
Path loss exponent (n)	1.6
Degree (g) in WCL method	0.5
Number of reference points (N)	20 and 32

- (a) Ranking: The means of the results of two or more algorithms are the same.
- (b) Post hoc with control method: The mean of the results of the control method and against each other groups is equal (compared in pairs).

The following tests are applied to the STAC web platform where it is assumed that the lower the result of an algorithm on a problem, the better of such algorithm [29].

- (i) Testbed 1 (corridor): here, we performed the tests for Wk-NN with 62 RPs, Wk-NN with 36 RPs, PF with 36 RPs, and WCL. Hence, the number of the group for the test (k) is four and the number of samples

(n) is nine (three different measurement places at three regions of the corridor). Moreover, the proposed method with 36 RPs is considered as the control method with a significance level (α) equal to 0.05.

The null hypothesis for ranking was rejected by the Friedman test with a p value of 0.00000. In addition, the null hypothesis for the post hoc test yielded the following results.

- (1) PF with 36 RPs versus WCL: H_0 is rejected with the p value of 0.00038.
- (2) PF with 36 RPs versus Wk-NN with 36 RPs: H_0 is rejected with the p value of 0.00697.
- (3) PF with 36 RPs versus Wk-NN with 62 RPs: H_0 is accepted with the p value of 0.85513.
- (ii) Testbed 2 (room): the ranking test is done for Wk-NN with 65 RPs, Wk-NN with 32 RPs, PF with 32 RPs, and WCL. Here, the number of the group for the test (k) is four and the number of samples (n) is three (three different measurement places inside the testbed room). The null hypothesis for ranking was rejected by the Friedman test with a p value of 0.01144. Similarly, the proposed method with 32 RPs is considered as the control method with a significance level (α) equal to 0.05. The null hypothesis for the post hoc test yielded the following results.
- (1) PF with 32 RPs versus WCL: H_0 is accepted with the p value of 0.08057.

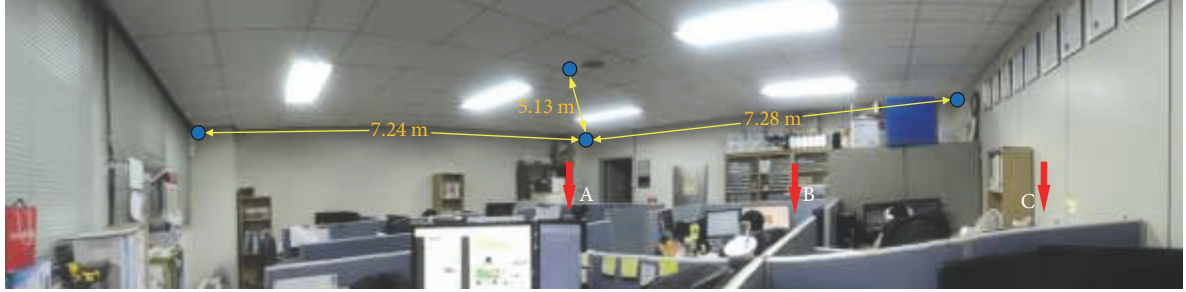


FIGURE 18: Panoramic view of the experimental environment: beacons deployed in the room where blue circular dots represent beacon deployment positions, and measurement places are marked with red arrows (A, B, and C).

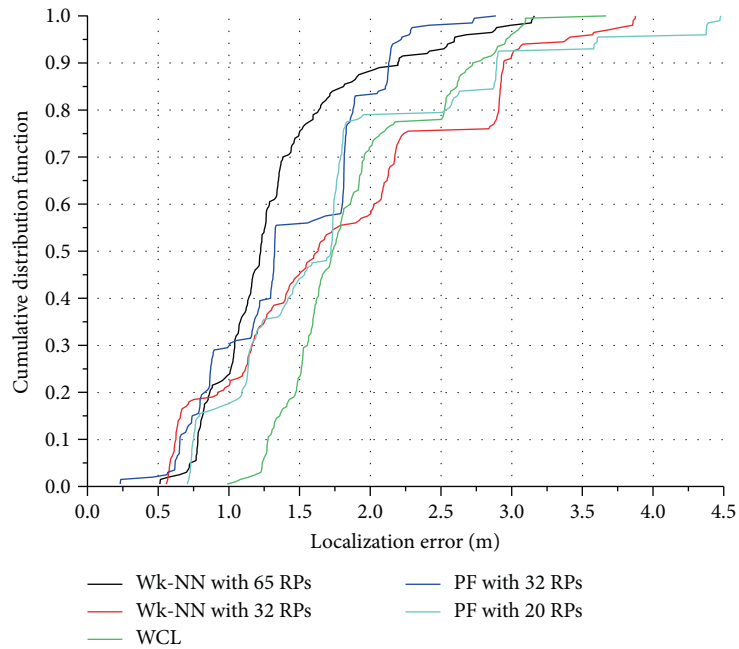


FIGURE 19: CDF of localization estimation error at a fixed place in testbed 2.

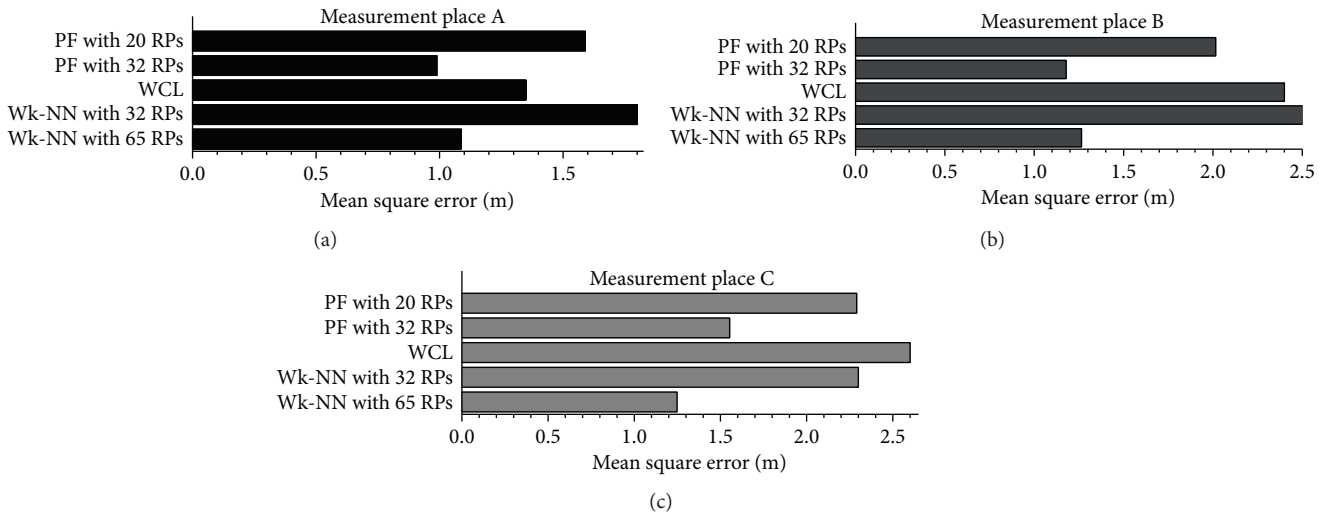


FIGURE 20: Average location error at different measurement places in the room: (a) measurement place A, (b) measurement place B, and (c) measurement place C. PF: proposed practical fingerprinting; Wk-NN: weighted k -nearest neighbor; WCL: weighted centroid localization; RF: reference points.

- (2) PF with 32 RPs versus Wk-NN with 32 RPs: H_0 is accepted with the p value of 0.11556.
- (3) PF with 32 RPs versus Wk-NN with 65 RPs: H_0 is accepted with the p value of 0.75783.

The null hypothesis for Friedman rank test is rejected at both the testbeds with a p value much lower than the significance level. Moreover, the null hypothesis for the post hoc tests compared in a pair of the proposed method and the Wk-NN (62 and 65 RPs) is accepted at both the testbeds with a p value much larger than the significance level. It signifies that performance of the proposed method differs from other methods, and the mean localization accuracy of the proposed technique is statistically similar to the existing Wk-NN fingerprinting approach.

5. Conclusion

The proposed fingerprinting method shows the reference points reduced for fingerprinting localization. We measured the performance of our method using various numbers of reference point cells over the localization area. We showed that it is possible to reduce the required number of reference point cells over a localization area using the traditional fingerprinting localization by joining it with another lateral approach to IPS. We used BLE as wireless technology to realize our proposed method of IPS. Since we use fewer reference points, the proposed method is less cumbersome and less time consuming than the traditional fingerprinting method. Moreover, the yielded location estimation is better than the location estimation by the WCL method when it is used solely.

Conflicts of Interest

The authors declare no conflict of interest.

Authors' Contributions

Santosh Subedi and Jae-Young Pyun conceived the idea and research metrology. Santosh Subedi designed the proposed localization algorithm and performed the experiments. Jae-Young Pyun contributed to the conception of the study and analysis by directing and supervising the research.

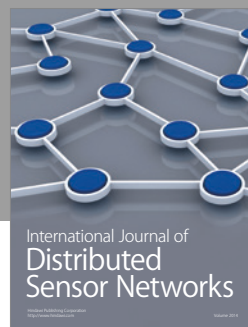
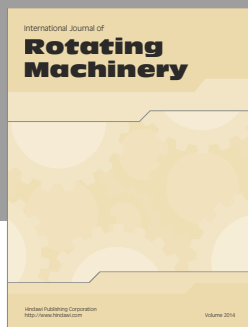
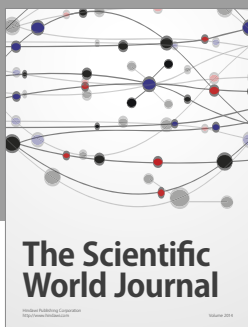
Acknowledgments

This work was supported by the Institute for Information & Communications Technology Promotion (IITP) grant funded by the Korea government (MSIT) (no. 2017-0-00695, Development by Hybrid Precision Indoor Positioning Commercial Technology for AR Indoor LBS) and the National Research Foundation of Korea (NRF) grant funded by the Korean Government (MOE) (no. NRF-2016R1D1A1B03935889).

References

- [1] R.-S. Cheng, W.-J. Hong, J.-S. Wang, and K. W. Lin, "Seamless guidance system combining GPS, BLE beacon, and NFC technologies," *Mobile Information Systems*, vol. 2016, Article ID 5032365, 12 pages, 2016.
- [2] S. Subedi, G.-R. Kwon, S. Shin, S.-s. Hwang, and J.-Y. Pyun, "Beacon based indoor positioning system using weighted centroid localization approach," in *2016 Eighth International Conference on Ubiquitous and Future Networks (ICUFN)*, Vienna, Austria, July 2016.
- [3] G. G. Anagnostopoulos and M. Deriaz, "Accuracy enhancement in indoor localization with the weighted average technique," in *Eighth International Conference on Sensor Technologies and Applications (SENSORCOMM)*, pp. 112–116, Lisbon, Portugal, November 2014.
- [4] P. Kriz, F. Maly, and T. Kozel, "Improving indoor localization using Bluetooth low energy beacons," *Mobile Information Systems*, vol. 2016, Article ID 2083094, 11 pages, 2016.
- [5] Z. Jianyong, L. Haiyong, C. Zili, and L. Zhaohui, "RSSI based Bluetooth low energy indoor positioning," in *2014 International Conference on Indoor Positioning and Indoor Navigation (IPIN)*, pp. 526–533, Busan, South Korea, October 2014.
- [6] F. Subhan, H. Hasbullah, A. Rozyev, and S. Bakhsh, "Indoor positioning in Bluetooth networks using fingerprinting and lateration approach," in *2011 International Conference on Information Science and Applications*, pp. 1–9, Jeju Island, South Korea, April 2011.
- [7] J. Blumenthal, R. Grossmann, F. Golatowski, and D. Timmermann, "Weighted centroid localization in ZigBee-based sensor networks," in *2007 IEEE International Symposium on Intelligent Signal Processing*, pp. 1–6, Alcala de Henares, Spain, October 2007.
- [8] A. Fink, H. Beikirch, M. Voss, and C. Schroeder, "RSSI-based indoor positioning using diversity and inertial navigation," in *2010 International Conference on Indoor Positioning and Indoor Navigation*, pp. 1–7, Zurich, Switzerland, September 2010.
- [9] S. Lee, B. Cho, B. Koo, S. Ryu, J. Choi, and S. Kim, "Kalman filter-based indoor position tracking with self-calibration for RSS variation mitigation," *International Journal of Distributed Sensor Networks*, vol. 2015, Article ID 674635, 2015.
- [10] P. Barsocchi, S. Chessa, A. Micheli, and C. Gallicchio, "Forecast-driven enhancement of received signal strength (RSS)-based localization systems," *ISPRS International Journal of Geo-Information*, vol. 2, no. 4, pp. 978–995, 2013.
- [11] Y. Kim, H. Shin, Y. Chon, and H. Cha, "Smartphone-based Wi-Fi tracking system exploiting the RSS peak to overcome the RSS variance problem," *Elsevier Pervasive and Mobile Computing*, vol. 9, no. 3, pp. 406–420, 2013.
- [12] X. Wang, L. Gao, S. Mao, and S. Pandey, "CSI-based fingerprinting for indoor localization: a deep learning approach," *IEEE Transactions on Vehicular Technology*, vol. 66, no. 1, pp. 763–776, 2017.
- [13] B. Sig, "Bluetooth Specification Version 4.0," 2010, <http://www.bluetooth.org>.
- [14] M. Siekkinen, M. Hiienkarj, J. K. Nurminen, and J. Nieminen, "How low energy is Bluetooth low energy? Comparative measurements with ZigBee/802.15.4," in *2012 IEEE Wireless Communications and Networking Conference Workshops (WCNCW)*, France, April 2012.

- [15] E. Dahlgren and H. Mahmood, *Evaluation of indoor positioning based on Bluetooth Smart technology*, [M.S. thesis], Department of Computer Science and Engineering, Chalmers University of Technology, Sweden, 2014.
- [16] R. Faragher and R. Harle, “Location fingerprinting with Bluetooth low energy beacons,” *IEEE Journal on Selected Areas in Communications*, vol. 33, no. 11, pp. 2418–2428, 2015.
- [17] A. Corbacho Salas, *Indoor Positioning System Based on Bluetooth Low Energy*, Universitat Politècnica de Catalunya, Barcelona, 2014.
- [18] <http://estimote.com/>.
- [19] S. He and S. H. Gray Chan, “Wi-Fi fingerprint-based indoor positioning: recent advances and comparisons,” *IEEE Communications Surveys and Tutorials*, vol. 18, no. 1, pp. 466–490, 2016.
- [20] M. Oussalah, M. Alakhras, and M. I. Hussein, “Multivariable fuzzy inference system for fingerprinting indoor localization,” *Fuzzy Sets and Systems*, vol. 269, pp. 65–89, 2015.
- [21] M. Zhou, Y. B. Xu, and L. Ma, “Radio-map establishment based on fuzzy clustering for WLAN hybrid KNN/ANN indoor positioning,” *China Communications*, vol. 7, no. 3, pp. 64–80, 2010.
- [22] H. Zhu and T. Alsharari, “An improved RSSI-based positioning method using sector transmission model and distance optimization technique,” *International Journal of Distributed Sensor Networks*, vol. 2015, Article ID 587195, 2015.
- [23] Y. Sung, “RSSI-based distance estimation framework using a Kalman filter for sustainable indoor computing environments,” *Sustainability*, vol. 8, no. 11, p. 1136, 2016.
- [24] V. Honkavirta, T. Perala, S. Ali-Loytty, and R. Piche, “A comparative survey of WLAN location fingerprinting methods,” in *2009 6th Workshop on Positioning, Navigation and Communication*, pp. 243–251, Hannover, Germany, March 2009.
- [25] K. Kaemarungsi and P. Krishnamurthy, “Modeling of indoor positioning systems based on location fingerprinting,” in *Twenty-third Annual Joint Conference of the IEEE Computer and Communications Societies*, vol. 2, pp. 1012–1022, Hong Kong, China, March 2004.
- [26] M. Friedman, “The use of ranks to avoid the assumption of normality implicit in the analysis of variance,” *Journal of the American Statistical Association*, vol. 32, pp. 674–701, 1937.
- [27] J. L. Hodges Jr. and E. L. Lehmann, “Ranks methods for combination of independent experiments in analysis of variance,” *The Annals of Mathematical Statistics*, vol. 33, pp. 482–497, 1962.
- [28] S. Holm, “A simple sequentially rejective multiple test procedure,” *Scandinavian Journal of Statistics*, vol. 6, pp. 65–70, 1979.
- [29] I. Rodríguez-Fdez, A. Canosa, M. Muñientes, and A. Bugarín, “STAC: a web platform for the comparison of algorithms using statistical tests,” in *Proceedings of the 2015 IEEE International Conference on Fuzzy Systems (FUZZ-IEEE)*, vol. 2–5, pp. 1–8, Istanbul Turkey, August 2015.



Hindawi

Submit your manuscripts at
<https://www.hindawi.com>

